Surgery 166 (2019) 1168–1175

Contents lists available at ScienceDirect

Surgery

journal homepage: www.elsevier.com/locate/surg

Breast

Mimetic sHDL nanoparticles: A novel drug-delivery strategy to target triple-negative breast cancer

Ton Wang, MD[a], Chitra Subramanian, PhD, MBA[a], Minzhi Yu, PhD[b], Peter T. White, MD[a], Rui Kuai, PhD[c], Jaquelyn Sanchez, BS[d], James J. Moon, PhD[b,e], Barbara N. Timmermann, PhD[f], Anna Schwendeman, PhD[b], Mark S. Cohen, MD, FACS[a,d,*]

[a] University of Michigan, Department of Surgery, Ann Arbor, MI
[b] University of Michigan, College of Pharmacy, Ann Arbor, MI
[c] Brigham and Women's Hospital, Department of Medicine, Boston, MA
[d] University of Michigan, Department of Pharmacology, Ann Arbor, MI
[e] University of Michigan, Department of Biomedical Engineering, Ann Arbor, MI
[f] University of Kansas, Department of Medicinal Chemistry, Lawrence, KS

ARTICLE INFO

Article history:
Accepted 10 June 2019
Available online 29 July 2019

ABSTRACT

Background: Withanolides are naturally derived heat shock protein 90 inhibitors that are potent in preclinical models of triple negative breast cancers. Conjugation to synthetic high-density lipoprotein nanoparticles improves solubility and targets delivery to the scavenger receptor B1. Triple negative breast cancers highly overexpress the scavenger receptor B1, and we hypothesize that encapsulation of the novel withalongolide A 4,19,27-triacetate by synthetic high-density lipoprotein will have enhanced efficacy against triple negative breast cancers in vivo.

Methods: Validated human triple negative breast cancer cell lines were evaluated for the scavenger receptor B1 expression by quantitative polymerase chain reaction and Western blot. Withalongolide A 4,19,27-triacetate inhibitory concentration$_{50}$ values were obtained using CellTiter-Glo assays (Promega, Madison, WI, USA). The scavenger receptor B1–mediated drug uptake was evaluated in vitro under fluorescence microscopy and in vivo with IVIS imaging of mouse xenografts (MD-MBA-468LN). To evaluate drug efficacy, mice were treated with synthetic high-density lipoprotein alone, withalongolide A 4,19,27-triacetate alone, withalongolide A 4,19,27-triacetate synthetic high-density lipoprotein, and chemotherapy or Prussian blue stain (control).

Results: Triple negative breast cancer cell lines had greater scavenger receptor B1 expression by quantitative polymerase chain reaction and Western blot versus controls. Fluorescent-labeled synthetic high-density lipoprotein uptake was scavenger receptor B1–mediated in vitro, and in vivo tumor uptake using IVIS imaging demonstrated significantly increased tumor radiant efficiency versus control. Inhibitory concentration$_{50}$ for withalongolide A 4,19,27-triacetate–treated cells with or without synthetic high-density lipoprotein encapsulation were 70-fold to 200-fold more potent than synthetic high-density lipoprotein alone. In triple negative breast cancer mouse xenografts, treatment with synthetic high-density lipoprotein withalongolide A 4,19,27-triacetate resulted in a 54% decrease in tumor volume compared with the control or with synthetic high-density lipoprotein alone.

Conclusion: The synthetic high-density lipoprotein withalongolide A 4,19,27-triacetate nanoconjugates are potent against triple negative breast cancers and show improved scavenger receptor B1–mediated targeting. Treatment with synthetic high-density lipoprotein–encapsulated withalongolide A 4,19,27-

Presented at the 2016 Academic Surgical Congress.

Ton Wang, MD and Chitra Subramanian contributed equally to this manuscript.

* Reprint requests: Mark S. Cohen MD, FACS, Professor of Surgery and Pharmacology, Director, Medical School Path of Excellence in Innovation and Entrepreneurship, Director of Endocrine Surgery Research, Department of Surgery, 2920K Taubman Center SPC 5331, University of Michigan Hospital and Health Systems, 1500 E. Medical Center Dr, Ann Arbor, MI 48109-5331, USA.
E-mail address: cohenmar@med.umich.edu (M.S. Cohen).

https://doi.org/10.1016/j.surg.2019.06.010

triacetate is able to significantly decrease the growth of tumor in mice compared with the control and has better efficacy than the current standard of care, warranting further evaluation as a novel therapeutic agent.

Introduction

More than 271,000 new diagnoses of invasive breast cancer have been predicted for 2019, making breast cancer the most commonly diagnosed cancer and the second leading cause of cancer-related death in women in the United States.[1] Substantial strides in screening, management of local tumor, adjuvant systemic therapy, and hormone/receptor therapies have resulted in decreasing the 5-y mortality rates during the past 3 decades.[2] Triple negative breast cancers (TNBCs) lack expression of the estrogen receptor (ER), progesterone receptor (PR), and human epidermal growth factor receptor 2 (HER-2/neu), creating a more aggressive subset of tumors that remain a challenge for clinicians to treat. These TNBCs account for ~10%–20% of invasive breast cancers.[3,4] and are associated with a more aggressive, basal-like subtype histopathology and BRCA1-related breast cancers.[5] The lack of ER, PR, and HER-2/neu renders hormonal and anti-HER-2/neu–targeted therapies essentially ineffective. Although TNBC has demonstrated increased chemosensitivity compared with ER-positive breast cancer, only 30%–45% receive a complete pathologic response because of the presence of residual disease after treatment.[6] An optimal selective systemic treatment thus far has not been identified, and first-line chemotherapy is based on combination therapy with anthracycline and taxane combinations, followed by capecitabine, cyclophosphamide, or—more recently—platinum-based compounds at the time of disease progression.[6–8]

Limited systemic treatments combined with the more aggressive TNBC phenotype results in decreased overall survival for patients with TNBCs compared with those patients with other types of breast cancer.[4,5] This problem highlights the need for the development of novel and efficacious therapies targeting these tumors. Although ER, PR, and HER-2/neu are not viable targets in TNBC, continued targeted research and molecular profiling has demonstrated promise in poly-adenosine phosphate ribose polymerase inhibitors, receptor tyrosine kinase inhibitors, mitogen-activated protein kinase inhibitors, phosphoinositide 3-kinase (PI3K)/Akt/mechanistic target of rapamycin (mTOR) inhibitors, heat shock protein 90 (HSP90) inhibitors, and Janus kinase/signal transducers and activators of transcription (JAK/STAT) inhibitors to name a few.[6,8] Although each of these holds potential as a future TNBC therapeutic, they remain in phase I/II/III clinical trials.

We demonstrated elsewhere[9] that withanolides are potent, novel inhibitors of HSP90 derived from natural plant sources in the *Solanacea* family and contain a 28-carbon steroidal lactone structure. Although these compounds have been shown in vivo to be highly efficacious in breast cancers,[9] challenges remain in their clinical translation attributable to their hydrophobicity, poor solubility in the plasma, and a circulation half-life of only 2–3 h. Our group previously mitigated these clinical limitations through developing a novel technique of nanoparticle drug delivery by encapsulating the poorly soluble withanolide, withalongolide A 4,19,27-triacetate (WGA-TA), with synthetic high-density lipoprotein (sHDL).[10] These 8–12 nM nanoparticles conferred improved circulation half-life and plasma solubility, and sHDL has been demonstrated as safe and well tolerated with minimal adverse reactions in phase III clinical trials.[11] HDL is naturally metabolized in the liver and binds to the scavenger receptor B1 (SR-B1), which mediates the uptake of selective HDL cholesteryl esters into the liver. It is important to note, SR-B1 is increasingly recognized as a biomarker and potential therapeutic target of multiple cancers including TNBC.[12–14] Because SR-B1 provides a target receptor for sHDL nanoparticles to bind, this facilitates uptake of cholesterol esters and anticancer drugs into the cytosol via a non-endocytic pathway, resulting in delivery of the encapsulated payload.[13,15] We hypothesized, therefore, that sHDL encapsulation of WGA-TA would specifically target high SR-B1–expressing TNBC cell lines resulting in enhanced delivery of the WGA-TA payload in vitro and in vivo.

Materials and Methods

Cell culture/reagents

The human normal female fibroblast (FF) and breast cancer cell lines SUM159, MDA-MB-231, MDA-MB-468LN (triple ER/PR and HER-2/neu negative), T47D, and MCF7 (both luminal A, ER^+) were validated by standard DNA fingerprinting techniques and 2-D cultured in high-glucose Dulbecco's modified Eagle medium (DMEM) (Life Technologies, Grand Island, NY, USA) supplemented with 10% fetal bovine serum (FBS) (Sigma-Aldrich, St. Louis, MO, USA), 100 U/mL penicillin and 100 μg/mL streptomycin (Life Technologies) according to our lab's previously published methods.[16] Jurkat cells were cultured in Roswell Park Memorial Institute 1640 (Thermo Fisher Scientific, Waltham, MA, USA) with 10% FBS and penicillin/streptomycin. NCI-H295R cells were cultured in 1:1 DMEM:F12 nutrient mixture (Thermo Fisher Scientific) supplemented with 10% FBS, penicillin/streptomycin, and insulin-transferrin-selenium (Thermo Fisher Scientific). Drug compounds utilized for these experiments included the novel HSP90/cdc37 inhibitor WGA-TA, which was isolated and purified in the laboratory of Dr Barbara Timmermann (University of Kansas, Lawrence, KS, USA), and sHDL nanoparticles, which were created in the laboratory of Dr Schwendeman (University of Michigan, Ann Arbor, MI, USA). The withanolide WGA-TA, a dialkylcarbocyanine lipophilic tracer dye (DiO), and the fluorescent dye 1,1′-Dioctadecyl-3,3,3′,3′ Tetramethylindotricarbocyanine Iodide (DiR) were loaded into sHDL nanoparticles, using methods as described elsewhere,[10] with the addition of DiO/DiR dye or WGA-TA during sHDL preparation. Control DiR-loaded liposomes (DiR-L) were created by dissolving 1,2-dimyristoyl-sn-glycero-3-phosphocholine (DMPC), 1-palmitoyl-2-oleoyl-sn-glycero-3-phosphocholine (POPC), and DiR in chloroform, which was removed subsequently by nitrogen flow and a vacuum oven to obtain the lipid film. The lipid film was hydrated with phosphate buffered saline ([PBS] pH 7.4) by bath and probe sonication to obtain DiR-L, which were diluted to 20 μg/mL by PBS for in vivo IVIS Spectrum imaging.

Cell proliferation assay

Equal numbers of FF, SUM159, MDA-MB-231, and MDA-MB-468LN cells were plated and left to adhere for 24 h in opaque, walled 96-well plates. Cells were then treated with serial concentrations of the study drugs sHDL, WGA-TA, and WGA-TA-sHDL at varying concentrations over 5 orders of magnitude. After 72 h of treatment, cell viability was assessed through adenosine triphosphate quantification, using the CellTiter-Glo luminescent cell

viability assay (Promega, Madison, WI, USA) according to the manufacturer's instructions. Briefly, CellTiter-Glo reagent was added to each well, mixed, and incubated at room temperature for 10 min. Luminescence was then read on a BioTek Synergy Neo plate reader using the Gen 52.01 software (BioTek, Winooski, VT, USA). The inhibitory concentration$_{50}$ (IC_{50}) values for sHDL, WGA-TA, and WGA-TA-sHDL in each of the cell lines were calculated using dose-response curves in GraphPad Prism (GraphPad Software, Inc, La Jolla, CA, USA).

Quantitative real-time polymerase chain reaction and Western blot analysis for SR-B1 expression

RNA from TNBC (SUM159, MDA-MB-231, MDA-MB-468LN), luminal A, ER^+ (MCF7 and T47D), negative controls (FF and Jurkat), and positive control (NCI-H295R) cell lines were extracted using a Qiagen RNA isolation kit (Qiagen Sciences, Valencia, CA, USA). Approximately 500 ng of RNA was reverse transcribed using a SuperScript Reverse Transcriptase kit from Life Technologies (Thermo Fischer Scientific). The quantitative polymerase chain reaction (qPCR) was performed in a StepOne real-time PCR (qPCR) system (Thermo Fischer Scientific), using SR-B1 and actin-specific primer sets. Relative gene expression levels were calculated after normalization with internal controls. Expression levels of SR-B1 were confirmed with Western blot analysis per our methods published elsewhere.[16] In brief, equal amounts of protein were loaded and separated using sodium dodecyl sulfate polyacrylamide gel electrophoresis (SDS-PAGE), transferred to nitrocellulose membrane, and blotted. We obtained SR-B1, donkey anti-rabbit IgG HRP (1:5000) and goat anti-mouse IgG HRP (1:5000) secondary antibodies from Santa Cruz Biotechnology (Santa Cruz, CA, USA) and β-Actin from EMD Millipore (Billerica, MA, USA). Actin levels were assessed to ensure equal loading and transfer of proteins. ImageJ software (National Institutes of Health, Bethesda, MD, USA) was used to obtain density of protein bands and results are described as normalized to actin expression.

The small interfering RNA knockdown of SR-B1 in SUM159 TNBC cells

Validated SR-B1 small interfering ribonucleic acid (siRNA) as well as nontargeting siRNA were transfected into SUM159 cells using Lipofectamine 2000 (Thermo Fisher Scientific) as per the manufacturer protocols. Then, 48 h post-transfection the cells were either collected for Western blot analysis or treated with sHDL-DiO for 4 h for subsequent uptake studies.

In vitro uptake of DiO-labeled sHDL nanoparticle

The TNBC cells lines SUM159, MDA-MB-231, MDA-MB-468LN, the negative control FF cells, and positive control NCI-H295R cells were incubated for 4 h with sHDL nanoparticles labeled with long-chain dialkylcarbocyanine lipophilic tracer DiO (Invitrogen, Thermo Fisher Scientific). To assess SR-B1–mediated uptake, cells were pretreated for 1 h with excess blank sHDL before the addition of sHDL-DiO nanoparticles. Cells were fixed in paraformaldehyde, nuclei stained with 4′, 6-diamidino-2-phenylindole, and fluorescent images obtained using a Nikon fluorescent microscope.

In vivo distribution of DiR-labeled sHDL nanoparticle in an MDA-MB468LN xenograft

Three million MDA-MB-468LN cells in 100 μL PBS were injected into the right posterior flank of athymic nude mice (Charles River, Skokie, IL). Once tumors reached 5–8 mm in diameter (approximately 6 weeks), mice were injected intraperitoneally with 0.6% DiR-labeled sHDL nanoparticle. After 24 h, whole body and organ fluorescent imaging and quantification of organs was performed, using the Xenogen IVIS Spectrum imaging system (Caliper Life Sciences, Hopkinton, MA, USA) at the University of Michigan Center for Molecular Imaging core facility.

In vivo evaluation of drug efficacy

Three million MDA-MB-468LN cells in 100 μL PBS were injected into the left mammary fat pad of athymic nude mice. Once the tumor size reached an approximate volume of 50mm^3, the mice were divided randomly into treatment groups of 4 mice each (PBS/control, sHDL, WGA-TA, WGA-TA-sHDL, or standard of care chemotherapy) for 21 days. The treatment groups received daily intraperitoneal injection of the drugs (200 μL PBS, 5 mg/kg WGA-TA, 5 mg/kg WGA-TA-sHDL, or an equivalent volume of sHDL). The mice in the chemotherapy group were treated with a combination of 2mg/kg doxorubicin and 100mg/kg cyclophosphamide once weekly. The mice were weighed 3 times weekly to assess general toxicity of the treatment, and tumor volumes were measured twice weekly with a digital caliper. Tumor volume was calculated using the formula: length $\times$ $(\text{width})^2$ /2. Posttreatment survival of the animals was followed for an additional 11 days at which point all mice were killed due to control mice reaching predetermined endpoints of tumor burden. All of the experiments involving mice were carried out in compliance with the University Committee on Use and Care of Animals at the University of Michigan.

Statistical analysis

Significance (set as 95%, $P < .05$) was determined using two-way ANOVA and Student's *t*-test. Best-fit normalized, dose-response curves for sHDL, WGA-TA, and WGA-TA-sHDL were used to calculate IC_{50} values with 95% confidence intervals in GraphPad Prism (GraphPad Software, Inc). Data are presented as mean values with error bars denoting standard deviation. Experiments were replicated in triplicate to ensure accuracy. Biostatistical data points were determined throughout the in vivo study, and tumor volumes and animal masses were calculated as mean ± standard error. Treatment differences with respect to tumor size were assessed via a 2-tailed Student's *t*-test. *P* values less than .05 in the *t*-test were considered statistically significant. The tumor volume progression/regression were plotted using GraphPad Prism software.

Results

SR-B1 is highly expressed on breast cancer cells

The sHDL nanoparticles are a natural ligand to the SR-B1 receptor. Increased expression of SR-B1 in target cancer cells is important for sHDL-drug conjugates to target these cells effectively and preferentially. We demonstrated that the TNBC cell lines SUM159, MDA-MB-231, and MDA-MB-468LN, as well as several luminal A, ER^+ cell lines (MCF7 and T47D), have increased expression of SR-B1 mRNA and protein compared with normal FF and Jurkat cells. Using qPCR compared with normal FF cells (controls), SR-B1 messenger ribonucleic acid (mRNA) expression was increased 3.2-fold in SUM159, 1.7-fold in MDA-MB-231, 9-fold in MDA-MB-468LN, 1.7-fold in MCF7, and 26-fold in T47D ($P < .05$ each). The mRNA expression for NCI-H295R cells, which are known to express high levels of SR-B1, was significantly increased 63.6-fold compared with FF cells and is shown as a positive control (Fig 1, *A*). This increased SR-B1 expression was confirmed by Western blot analysis, which demonstrated statistically significantly increased SR-B1 protein levels in SUM159, MDA-MB-468LN, and MCF7 cell

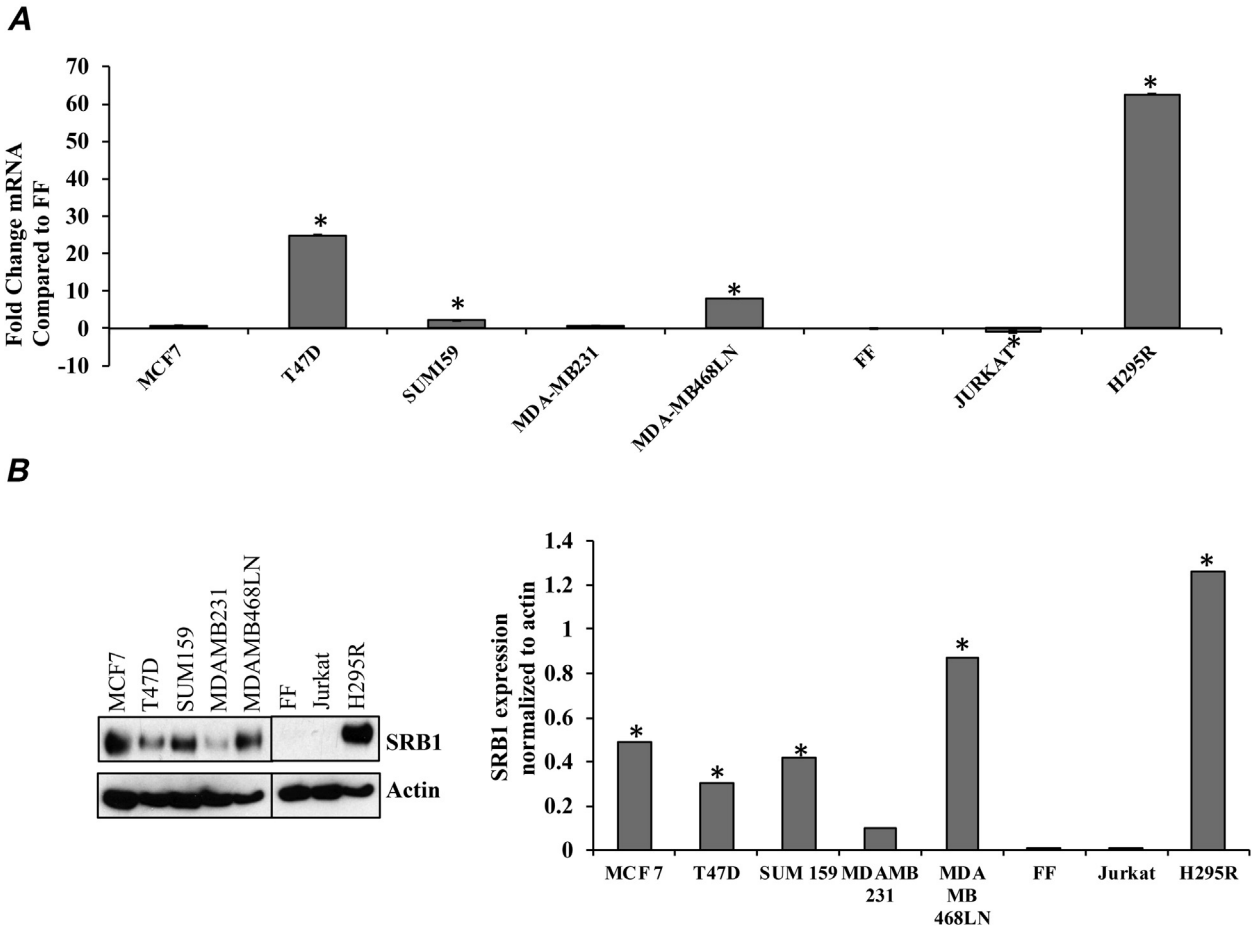

Fig 1. (*A*) Quantitative polymerase chase reaction (qPCR) levels of scavenger receptor B1 (SR-B1) mRNA in several breast cancer cell lines, including luminal A, ER^+ cell lines and triple negative breast cancer (TNBC) cells. Compared with normal female fibroblast (FF) cells, there are 1.7-fold and 26.0-fold increased in mRNA expression for MCF7 and T47D, respectively, and 3.2-fold, 1.7-fold, and 9.0-fold increased mRNA expression in TNBC cells lines SUM159, MDA-MB-231, and MDA-MB-468LN, respectively ($P < .05$) (*B*) Western blot analysis of SR-B1 protein expression. Increased protein expression in MCF7, SUM159, and MDA-MB-468LN breast cancer cell lines. $^*P < .05$. (*C*) Densitometric analysis of SR-B1 protein expression relative to actin.

lines with a trend towards significance for MDA-MB-231 ($P = .08$), and T47D ($P = .06$; Fig 1, *B* and *C*).

SR-B1 receptor modulates uptake of DiO-sHDL conjugated nanoparticles

SR-B1 functions to internalize HDL during normal metabolism of cholesterol. To assess the role of SR-B1 in mediating the uptake of the sHDL nanoparticle cargo, we used DiO dye conjugated to sHDL nanoparticles. Positive control (high SR-B1 expressing NCI-H295R cells), negative control (FF cells), and TNBC cell lines SUM159, MDA-MB-231 and MDA-MB-468LN were incubated with DiO-sHDL for 4 h, with or without 1 h of excess sHDL pretreatment. The uptake of the DiO dye was then captured by fluorescent microscopy (Fig 2, *A*). The amount of DiO uptake into the cells correlated with the levels of SR-B1 expression identified in Figure 1 with minimal uptake of the green DiO dye in FF cells, increased uptake in highly SR-B1 expressing NCI-H295R cells, and uptake in all 3 TNBC cell lines. In addition, pretreatment with excess sHDL in all the cell lines and siRNA against SR-B1 in SUM159 (Fig 2, *B*) completely blocked DiO uptake into the cells, which indicates that the SR-B1 receptor likely plays a key role in modulating the internalization of the sHDL nanoparticles and their cargo. Knock down of SRB1 protein was verified using immune blot analysis (Fig 2, *C*).

Cell viability/proliferation

The effect of sHDL and WGA-TA alone or after WGA-TA encapsulation with sHDL on cell viability was determined using CellTiter-Glo luminescent cell viability assays. The half maximal IC_{50} was determined from dose-response curves (Fig 3) and reported in the Table. Treatment with sHDL alone had minor effects on cell viability, with an IC_{50} value >24 μM for FF cells, and ranging 7.1–20.5 μM for TNBC cells. Treatment with WGA-TA was highly potent, with TNBC IC_{50} values ranging 10.3–68 nM. This drug effect in the TNBC cells demonstrated a greater than 5-fold increased potency over treatment in FF cells. Although encapsulation of WGA-TA with the mimetic sHDL slightly increased the IC_{50} values across all cells lines, the drug still maintained statistically significant potency in TNBCs compared with FF cells.

Increased in vivo TNBC xenograft uptake of DiR-sHDL nanoparticles

We next examined the whole body and organ distribution of sHDL nanoparticle after treatment using MDA-MB-468LN xenografts in athymic nude mice. Conjugated DiR-sHDL was injected intraperitoneally, and the distribution of DiR was determined after 24 h, using the IVIS Spectrum imaging. Control mice were injected with nonspecific DiR-liposome. The whole body distribution (Fig 4, *A*) identified increased uptake of DiR-sHDL in the MDA-MB468LN

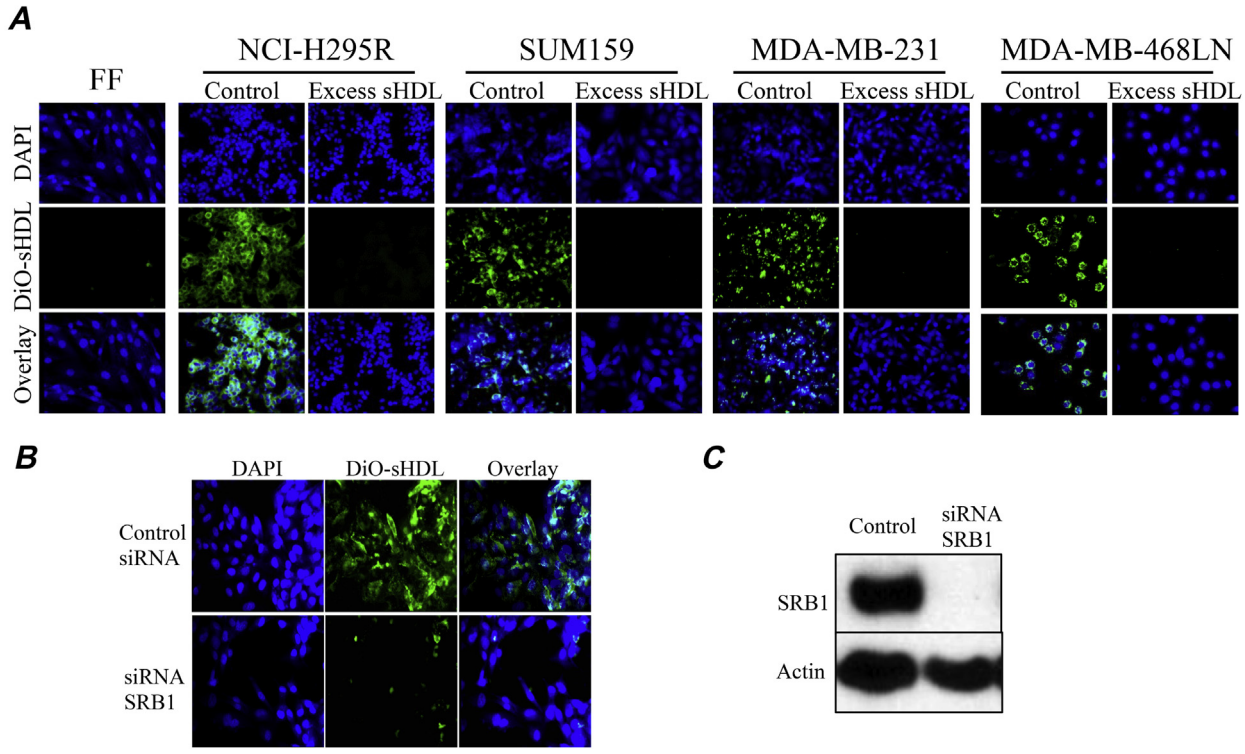

Fig 2. (*A*) TNBC cell lines were treated for 4 h with DiO-sHDL conjugated nanoparticles with or without 1 h of excess sHDL pretreatment. Minimal uptake of DiO dye occurred in FF cells; whereas the uptake increased in all three TNBC cell lines. This uptake was blocked completely by sHDL pretreatment. Level of DiO uptake corresponds to the level of SR-B1 expression presented in Fig 1. (*B*) Pretreatment with small interfering RNA (siRNA) to SR-B1 in SUM159 cells also completely abolished DiO uptake. (*C*) The siRNA against SR-B1. SR-B1 expression is abolished completely with siRNA treatment.

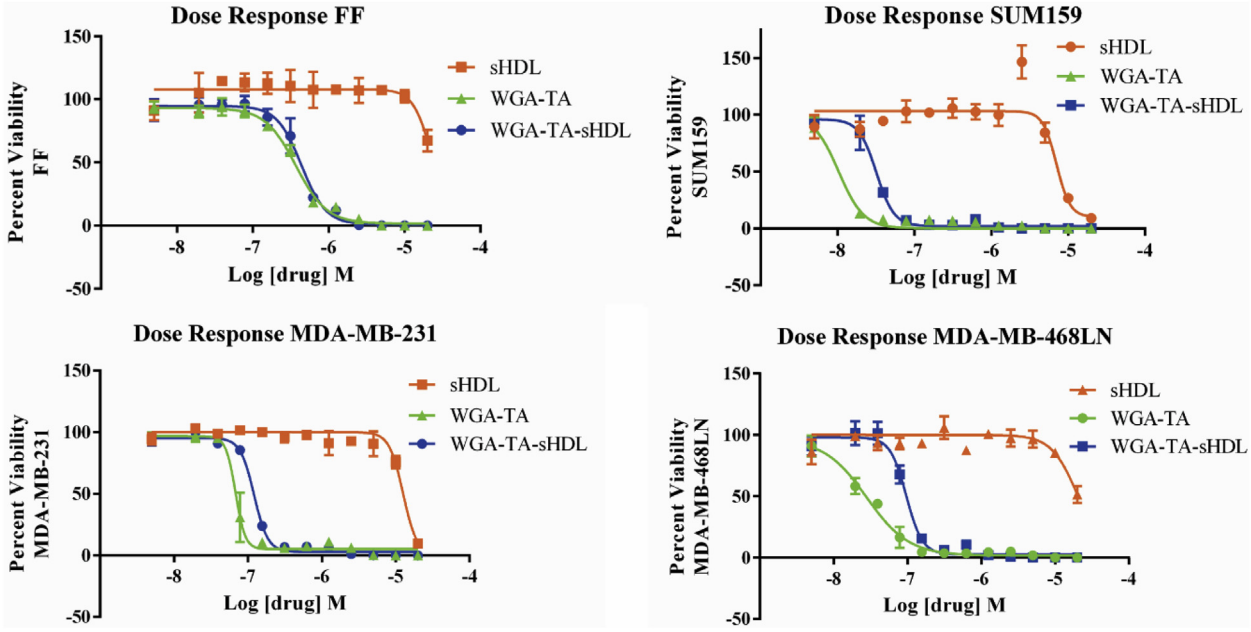

Fig 3. Dose-response curves of normal female fibroblasts (FF) and the three TNBC cell lines. The half maximal inhibitory concentration (IC_{50}) was determined using a best-fit curve. The Table reports the IC_{50} values, in which WGA-TA–treated cells had IC_{50} concentrations ranging from 10 to 121 nM that were 70-fold to 200-fold more potent than cells treated with sHDL alone (IC_{50} 7 to 24 μM). TNBCs were 5 times more sensitive to WGA-TA treatment than normal fibroblasts.

tumors compared with controls at 24 h. After the animals were killed, a necroscopy was performed, and individual organ imaging of brain, heart, lung, spleen, kidneys, liver, and tumor was performed (Fig 4, *B*), there was a significant increase in DiR uptake in the high SR-B1 expressing MDA-MB-468LN tumors compared with the controls ($P < .001$). Although there was also increased uptake in the heart, lung, and kidney, this uptake was relatively minor. Both control and DiR-sHDL mice had increased uptake in the spleen and

Table
Antiproliferative activity of sHDL, WGA-TA, and WGA-TA-sHDL against human triple negative breast cancer cells

Cell line	sHDL	WGA-TA	WGA-TA-sHDL
FF	>24.4 μM	370 nM (337–406)	438 nM (396–484)
SUM159	7.1 μM (5.4–9.2)	10.3 nM (9.3–11.5)	32 nM (29.7–34.6)
MDA-MB-231	12.6 μM (11.8–13.6)	68.0 nM (59.9–77.2)	121 nM (115–128)
MDA-MB-468LN	20.5 μM (17.3–24.3)	27.8 nM (23.1–33.5)	96 nM (88.5–104)

NOTE: Results presented as the half maximal inhibitory concentration (IC_{50}) with 95% confidence intervals.

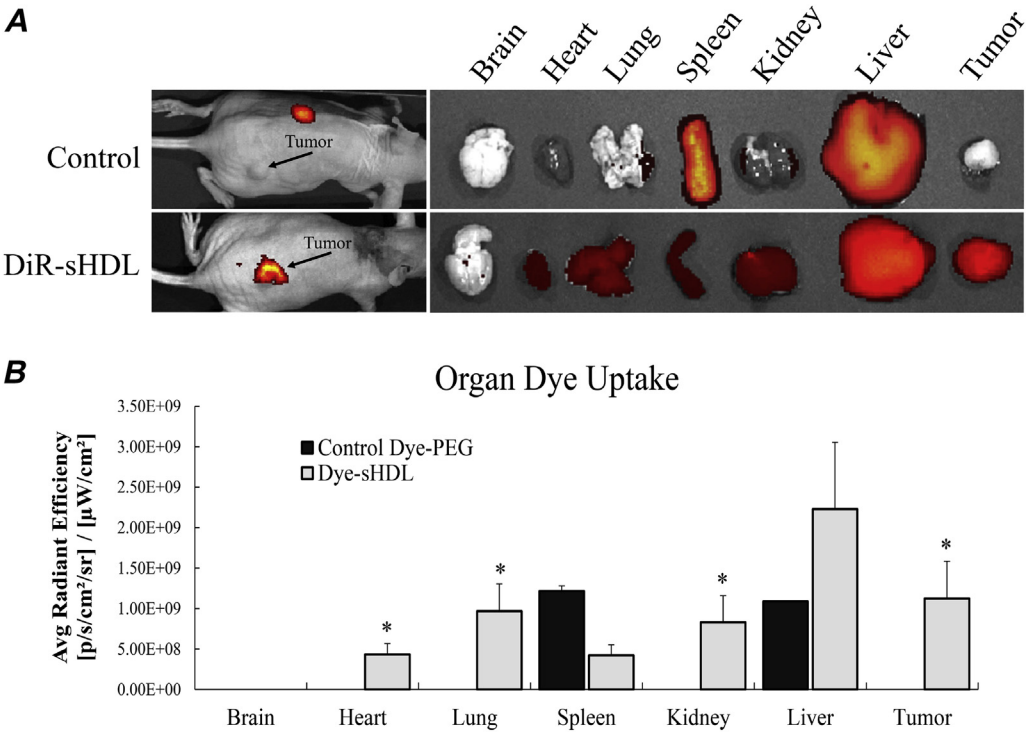

Fig 4. (*A*) Whole body and organ distribution of DiR-sHDL nanoparticle in a MDA-MB-468LN mouse xenograft model. Mice were injected intraperitoneally, then imaged 24 h later using IVIS Spectrum. Control mice received an injection of DiR-liposome (DiR-L). (*B*) Graph of the average radiant efficiencies of brain, heart, lung, spleen, kidneys, liver, and tumor. There were undetectable levels in all control organs except for spleen and liver. There is a statistically significant increase in DiR uptake in the MDA-MB-468LN tumors, as well as a more limited uptake in the heart, lung, and kidney of DiR-sHDL mice.

liver, which is expected, because the reticuloendothelial system is a known aggregation site for nanoparticles, and the liver naturally expresses SR-B1 for the metabolism of cholesterol.

WGA-TA-sHDL is effective at suppressing breast cancer tumor growth in vivo

Approximately 3 million MDA-MB-468LN cells were injected into the mammary fat pad of nude mice. Once the tumors reached 50 mm^3, the mice were treated with PBS (control), sHDL, WGA-TA, WGA-TA-sHDL, or standard-of-care chemotherapy (doxorubicin plus cyclophosphamide) for 21 days. As shown in Figure 5, at the end of the treatment period, tumor volumes for the mice treated with sHDL and chemotherapy were equivalent to that of control mice, and tumor volumes for mice treated with WGA-TA and WGA-TA-sHDL were 59% ($P = .02$) and 50% ($P = .04$), respectively, that of the control mice. At the end of the study (11 days after the end of treatment), tumor volumes for the mice treated with sHDL were again equivalent to that of the control mice, and tumor volumes for the mice treated with WGA-TA, WGA-TA-sHDL, and chemotherapy were 80% ($P = 0.27$), 46% ($P = 0.03$), and 69% ($P = .10$), respectively, that of the control mice. When comparing the different treatment groups, the tumor volumes for the mice treated with WGA-TA-sHDL were smaller than the tumors treated with sHDL alone ($P = .05$) and trended toward being smaller compared with tumors treated with WGA-TA alone ($P = .06$). The tumor volumes were no different with WGA-TA-sHDL treatment compared with chemotherapy ($P = .15$).

Toxicity was assessed by evaluating the average percent change in body weight. As seen in Figure 6, the mice treated with WGA-TA and WGA-TA-sHDL experienced weight loss during the course of treatment. At the end of the treatment period, the mice treated with WGA-TA and WGA-TA-sHDL experienced approximately 7% and 6% body weight loss, respectively ($P < .05$ for WGA-TA compared with the control mice); however, after stopping injections, the weights of all the mice rebounded quickly, and there were no differences in weight in all treatment groups.

Discussion

TNBC remains a difficult malignancy to treat, because only 30%–45% of patients treated with conventional systemic chemotherapy

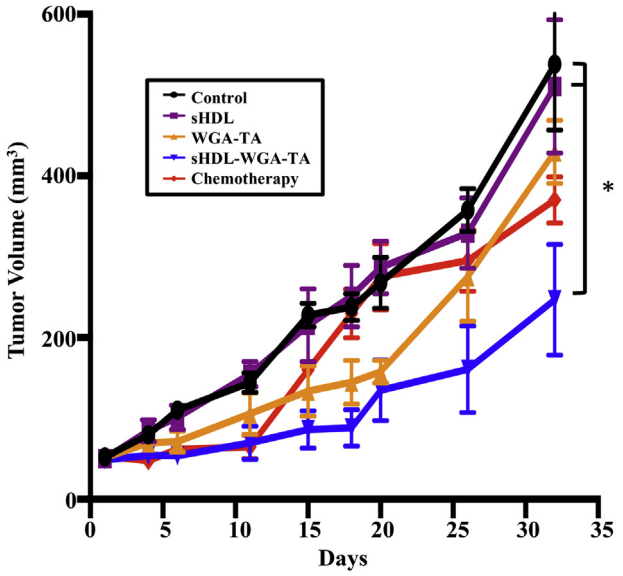

Fig 5. Approximately 3 million MDA-MB-468LN cells were injected in the mammary fat pad of nude mice. Once the tumors reached approximately 50 mm^3, the mice were treated for 21 days with PBS (control), sHDL, WGA-TA, WGA-TA-sHDL, or chemotherapy (doxorubicin plus cyclophosphamide). At the end of the study, tumor volumes for mice treated with sHDL, WGA-TA, WGA-TA-sHDL, and chemotherapy were 95% ($P = .82$), 80% ($P = .27$), 46% ($P = .03$), and 69% ($P = .10$), respectively, that of the control mice.

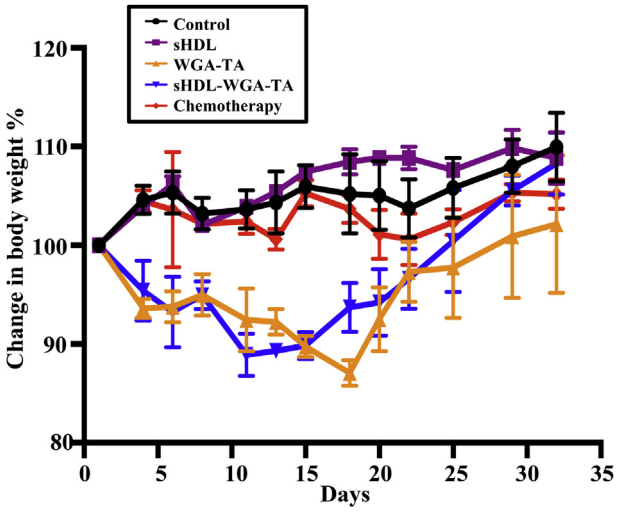

Fig 6. Toxicity was assessed by evaluating the average percent change in body weight. Mice treated with WGA-TA and WGA-TA-sHDL experienced weight loss during treatment; however, after stopping injections, all mice regained weight rapidly and no differences in weight were observed in all treatment groups.

achieve complete pathologic responses, leaving the majority of patients with ongoing disease and poor clinical outcomes.[4] Given the critical need for better treatments for this disease, there are now a number of promising new targeted therapies aimed at inhibiting one or more oncogenic or proliferative pathways in TNBC that are still in clinical trials, including new poly-adenosine phosphate ribose polymerase inhibitors, HSP90 inhibitors, and checkpoint inhibitors.[6]

A recent targeted strategy for TNBC is based on the identification of increased SR-B1 expression in TNBCs.[13,14] Although HDL and its mimetic sHDL bind effectively to the SR-B1 receptor, this lipoprotein by itself is not potent against breast cancers. Applying the strategy of using sHDL to carry a drug payload to cells overexpressing SR-B1 is a therapeutic concept that has been shown effective in adrenocortical cancers.[10] Therefore, we chose to use this same strategy in TNBCs, because WGA-TA is a potent inhibitor of these cells in vitro. The main difficulties in translating this natural withanolide in vivo have been its relatively hydrophobic nature that limits its solubility, as well as a short, 2- to 3-h half-life in serum. To both improve the pharmacokinetic profile of WGA-TA and provide enhanced drug delivery to highly expressing SR-B1 TNBC tumors, our group has developed a method of encapsulating WGA-TA in sHDL nanoparticles.[10] In this study, we show that encapsulation of WGA-TA in sHDL does not dramatically alter the drug potency, because the IC_{50} values remained <121 nM in TNBC, still several-fold more selective than normal fibroblast cells. The majority of this effect is likely representative of WGA-TA-sHDL uptake being influenced by levels of SR-B1 expression and of the imperfect (85%) yield of WGA-TA during encapsulation in sHDL. As such, the WGA-TA concentration is likely 15%–20% less in WGA-TA-sHDL than the unencapsulated WGA-TA drug, which would account for most of the effect of the slightly greater WGA-TA-sHDL IC_{50} values we observed.

SR-B1 receptor is not only a cancer biomarker but is also tied to the activation of several prosurvival and oncogenic pathways.[14,17] Expression of SR-B1 has been associated recently with invasive ductal breast cancer, more aggressive tumor behavior, and worse overall survival.[18] These findings have set the stage for using synthetically customized HDL nanoparticles to target SR-B1 and deliver cytotoxic payloads in a number of malignancies, including breast, prostate, ovarian, hepatic, neuroblastoma, lymphoma, and adrenal cancers.[10,15,19,20] In breast cancer, paclitaxel loaded into discoidal, reconstituted, HDLs has demonstrated improved targeting, cytotoxicity, and limitation of tumor growth compared with unmodified paclitaxel.[20] Loading small interfering RNA molecules into reconstituted HDL has also shown enhanced SR-B1 tumor-selective targeting, cytosolic delivery through a non-endocytotic mechanism to bypass endo-lysomal trapping, with enhanced antitumor effects in breast cancer.[21] In our study, we demonstrated that TNBC has a 1.7-fold to 9.0-fold increase in SR-B1 expression compared with normal fibroblast cells, and that several luminal A, ER^+ cell lines also have increased SR-B1 expression. By exploiting this increased expression over normal cells, sHDL encapsulation increased payload delivery to TNBC cells as demonstrated by increased dye uptake both in vitro and in vivo. This process is clearly SR-B1 mediated, because excess sHDL and siRNA pretreatment effectively blocked this uptake. In MDA-MB-468LN xenografts, sHDL encapsulation increased tumor targeting compared with a nonspecific, liposome drug delivery system.

In light of these findings, our study demonstrated the use of a synthetically developed HDL nanoparticle that was created to improve the pharmacokinetics of WGA-TA and to enhance targeting and delivery of cytotoxic drug payloads via SR-B1 expression in breast cancer. We demonstrated that conjugation of WGA-TA with sHDL is able to decrease growth of the breast cancer tumor in vivo after treatment for 21 days, an effect that appears durable after discontinuation of drug administration. Of note, without nanoparticle encapsulation of WGA-TA, WGA-TA alone is unable to deliver the same antitumor effect observed with WGA-TA-sHDL. In addition, unlike in other cancer models, such as in nasopharyngeal cancer, the sHDL particle alone did not demonstrate any antitumor effect through SR-B1 targeting.[12] The WGA-TA-sHDL treatment resulted in superior efficacy compared with the current standard of care, which is combination cytotoxic chemotherapy with doxorubicin and cyclophosphamide. Although the mice treated with WGA-TA and WGA-TA-sHDL experienced mild weight loss, they regained weight quickly after the cessation of drug administration.

Further steps in this investigation would include a large-scale translational animal study with patient-derived xenografts. Additionally, it would be exciting to evaluate possible synergistic effects of these agents in combination with standard-of-care chemotherapy drugs for treatment of TNBC.

In conclusion, withanolides have shown a remarkable therapeutic index with high potency in cancer cells. Their challenge in clinical development and application has been their hydrophobicity, poor solubility in serum, and rapid clearance with a half-life of only 2–3 h. Conjugation of these withanolides with sHDL appears to solve this issue of solubility, and improving the half-life through its sustained-release effect (data not presented) and providing an improved tumor cell targeting delivery strategy through the SR-B1 receptor. The current study demonstrated that WGA-TA-sHDL conjugation is a potent, anticancer strategy in vitro and in vivo in TNBCs that targets these tumors selectively and effectively, demonstrating early promise for further translational evaluation.

Funding/Support

This work was partially funded by the National Institutes of Health (T32 CA009672, R01 CA173292), NIH 3U01-CA-120458-03, Coller Surgical Society Research Fellowship, the University of Michigan Rogel Comprehensive Cancer Center, United States Support Grant P30-CA-046592, and the University of Michigan Department of Surgery.

Conflict of interest/Disclosure

The authors report no proprietary or commercial interest in any product mentioned or concept discussed in this article.

References

1. American Cancer Society. Cancer Facts & Figures 2019. Web site. https://www.cancer.org/content/dam/cancer-org/research/cancer-facts-and-statistics/annual-cancer-facts-and-figures/2019/cancer-facts-and-figures-2019.pdf. Accessed March 1, 2019.
2. Howlader N, Noone AM, Krapcho M, et al. SEER Cancer Statistics Review, 1975–2013, National Cancer Institute. Web site http://seer.cancer.gov/csr/1975_2013/. Accessed March 1, 2019.
3. Boyle P. Triple-negative breast cancer: Epidemiological considerations and recommendations. *Ann Oncol*. 2012;23(suppl 6):vi7–vi12.
4. Liedtke C, Mazouni C, Hess KR, et al. Response to neoadjuvant therapy and long-term survival in patients with triple-negative breast cancer. *J Clin Oncol*. 2008;26:1275–1281.
5. Brown M, Tsodikov A, Bauer KR, Parise CA, Caggiano V. The role of human epidermal growth factor receptor 2 in the survival of women with estrogen and progesterone receptor-negative, invasive breast cancer: The California Cancer Registry, 1999–2004. *Cancer*. 2008;112:737–747.
6. Kalimutho M, Parsons K, Mittal D, López JA, Srihari S, Khanna KK. Targeted therapies for triple-negative breast cancer: Combating a stubborn disease. *Trends Pharmacol Sci*. 2015;36:822–846.
7. Denduluri N, Somerfield MR, Eisen A, et al. Selection of optimal adjuvant chemotherapy regimens for human epidermal growth factor receptor 2 (HER2) -negative and adjuvant targeted therapy for HER2-positive breast cancers: An American Society of Clinical Oncology Guideline Adaptation of the Cancer Care Ontario Clinical Practice Guideline. *J Clin Oncol*. 2016;34:2416–2427.
8. Crown J, O'Shaughnessy J, Gullo G. Emerging targeted therapies in triple-negative breast cancer. *Ann Oncol*. 2012;23(suppl 6):vi56–vi65.
9. Zhang X, Timmermann B, Samadi AK, Cohen MS. Withaferin a induces proteasome-dependent degradation of breast cancer susceptibility gene 1 and heat shock factor 1 proteins in breast cancer cells. *ISRN Biochem*. 2012;2012:707586.
10. Subramanian C, Kuai R, Zhu Q, et al. Synthetic high-density lipoprotein nanoparticles: A novel therapeutic strategy for adrenocortical carcinomas. *Surgery*. 2016;159:284–294.
11. Kuai R, Li D, Chen YE, Moon JJ, Schwendeman A. High-density lipoproteins: Nature's multifunctional nanoparticles. *ACS Nano*. 2016;10:3015–3041.
12. Zheng Y, Liu Y, Jin H, et al. Scavenger receptor B1 is a potential biomarker of human nasopharyngeal carcinoma and its growth is inhibited by HDL-mimetic nanoparticles. *Theranostics*. 2013;3:477–486.
13. McMahon KM, Foit L, Angeloni NL, Giles FJ, Gordon LI, Thaxton CS. Synthetic high-density lipoprotein-like nanoparticles as cancer therapy. *Cancer Treat Res*. 2015;166:129–150.
14. Danilo C, Gutierrez-Pajares JL, Mainieri MA, Mercier I, Lisanti MP, Frank PG. Scavenger receptor class B type I regulates cellular cholesterol metabolism and cell signaling associated with breast cancer development. *Breast Cancer Res*. 2013;15:R87.
15. Foit L, Giles FJ, Gordon LI, Thaxton CS. Synthetic high-density lipoprotein-like nanoparticles for cancer therapy. *Expert Rev Anticancer Ther*. 2015;15:27–34.
16. Grogan PT, Sleder KD, Samadi AK, Zhang H, Timmermann BN, Cohen MS. Cytotoxicity of withaferin A in glioblastomas involves induction of an oxidative stress-mediated heat shock response while altering Akt/mTOR and MAPK signaling pathways. *Invest New Drugs*. 2013;31:545–557.
17. Cruz PM, Mo H, McConathy WJ, Sabnis N, Lacko AG. The role of cholesterol metabolism and cholesterol transport in carcinogenesis: A review of scientific findings, relevant to future cancer therapeutics. *Front Pharmacol*. 2013;4:119.
18. Li J, Wang J, Li M, Yin L, Li X-A, Zhang T-G. Up-regulated expression of scavenger receptor class B type 1 (SR-B1) is associated with malignant behaviors and poor prognosis of breast cancer. *Pathol Res Pract*. 2016;212:555–559.
19. Yang S, Damiano MG, Zhang H, et al. Biomimetic, synthetic HDL nanostructures for lymphoma. *Proc Natl Acad Sci U S A*. 2013;110:2511–2516.
20. Wang J, Jia J, Liu J, He H, Zhang W, Li Z. Tumor targeting effects of a novel modified paclitaxel-loaded discoidal mimic high density lipoproteins. *Drug Deliv*. 2013;20:356–363.
21. Ding Y, Wang Y, Zhou J, et al. Direct cytosolic siRNA delivery by reconstituted high density lipoprotein for target-specific therapy of tumor angiogenesis. *Biomaterials*. 2014;35:7214–7227.